ICIP 2019

"A dual attention dilated residual network for liver lesion classification and localization on CT images "

Xiao Chen, Lanfen Lin, Yen-Wei Chen, et al.

Zhejiang University, Ritsumeikan University, Sir Run Run Shaw Hospital

RITSUMEIKAN

Content

Introduction

Backgrounds

Liver cancer is the second most common cause of cancer-related deaths among men and sixty among women.

Major concern limits automatic liver lesion classification is that previous methods are conducted on lesion level, which relies heavily on ROI selection process.

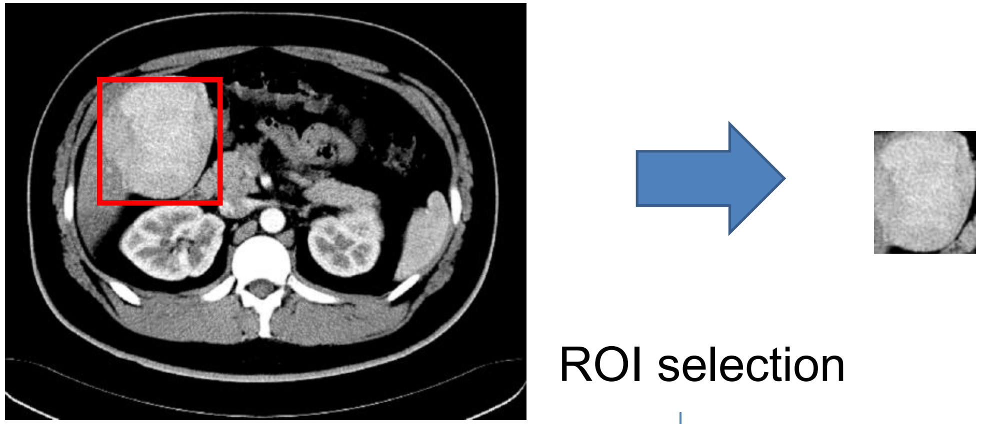

ROI selection

- Labor-intensive Manual annotations
- Automatic lesion detection/segmentation

Motivation

To relieve the burden of expensive pixel-level lesions' annotations, we first explored the potential of using the whole liver slice image for liver lesion classification without pre- detection or pre-selection of the ROI.

ART Phase

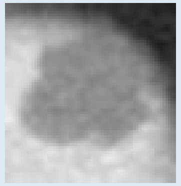

Previous methods:

1. segment liver lesions
2. conduct lesion-level classification
   (ROI-level, patch-level, or both)

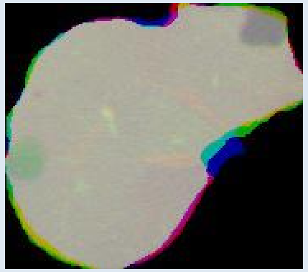

Our proposed methods:

1. segment whole liver area
2. conduct image-level classification
   (without lesion detection or segmentation)

Motivation

Contributions

- Our proposed DADRN framework no longer relies on lesion annotations and could tackle the lesion classification problem as a one-stage process.
- Our dual-attention mechanism integrates similar features of high-level feature map from a global view, which improves DRN’s lesion recognition performance
- The experimental results show that DADRN is comparable to the ROI-level classification model and is superior to other state-of-the-art attention-based classification models in lesion classification task and weakly- supervised lesion localization task.

Motivation

Related Work

- Attention mechanism in Computer Vision

Squeeze-Excitation block[1]

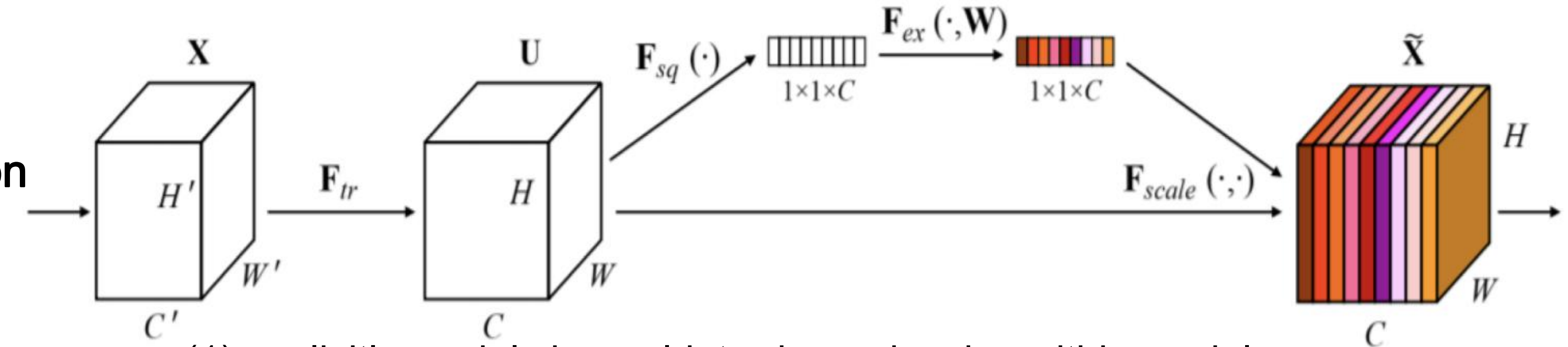

(1) explicitly model channel-interdependencies within modules

Dual Attention block[2]

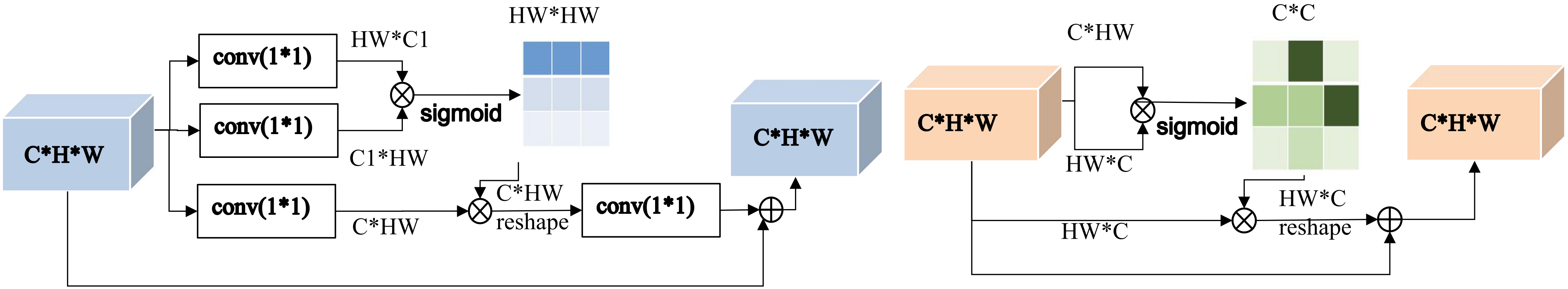

a. spatial attention block

b. channel attention block

(2) model long-range dependencies and capture concurrent features within modules

[1] Hu, Jie, Li Shen, and Gang Sun. "Squeeze-and-excitation networks." Proceedings of the IEEE conference on computer vision and pattern recognition. 2018.
[2] Wang, Xiaolong, et al. "Non-local neural networks." Proceedings of the IEEE Conference on Computer Vision and Pattern Recognition. 2018.

➢ Closer look to dual attention block

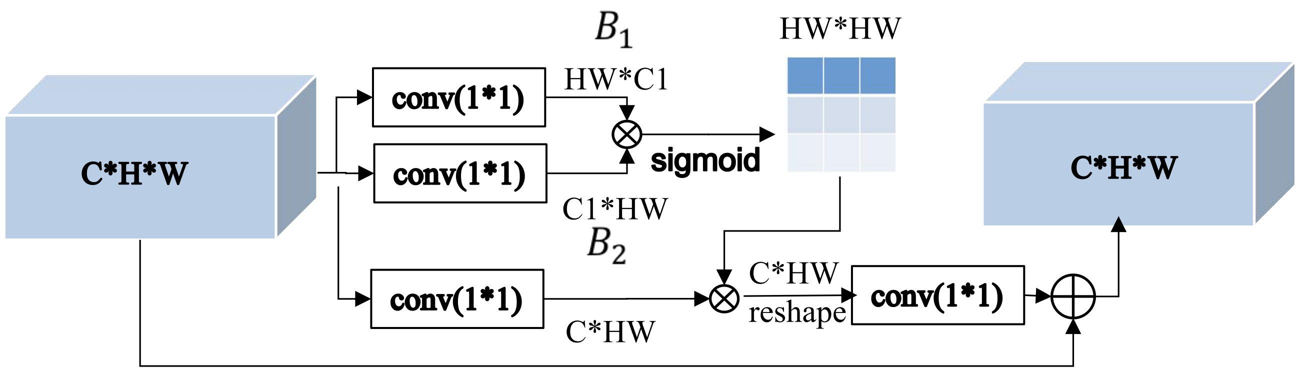

a. spatial attention block [1]

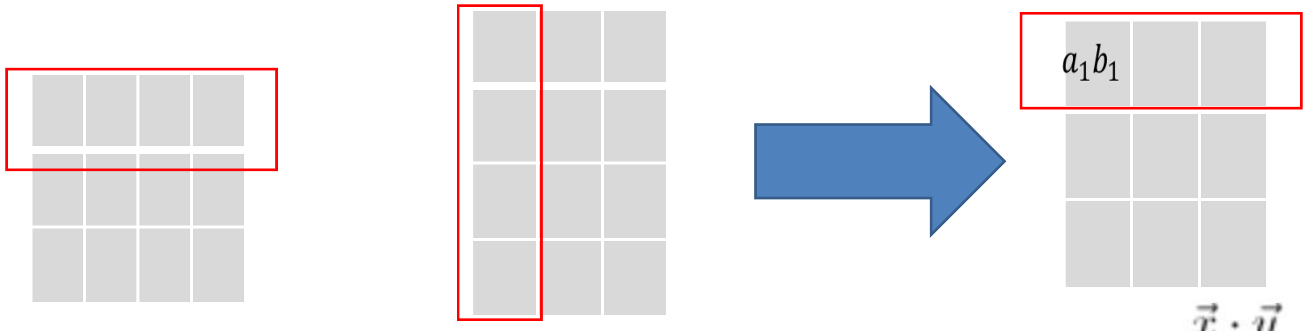

$$sim(X, Y) = cos\theta = \frac{\vec{x} \cdot \vec{y}}{||x|| \cdot ||y||}$$

b. Illustration of step1 batch matrix multiplication

Step1: Batch matrix multiplication

$$S_{ij} = {B_1}^T B_2$$

Step2: Normalize similarity map

$$\alpha_{ji} = \frac{1}{1+e^{-S_{ij}}},$$

Step3: Synthesize new feature map

$$o_j = \sum_{i=1}^{N} \alpha_{j,i} D_i$$

Step4: Adaptively learn the weight of synthesized feature map

$$y_j = \beta o_j + A_j$$

[1]: Wang, Xiaolong, et al. "Non-local neural networks." Proceedings of the IEEE Conference on Computer Vision and Pattern Recognition. 2018.

Content

Methodology

Overview of my research

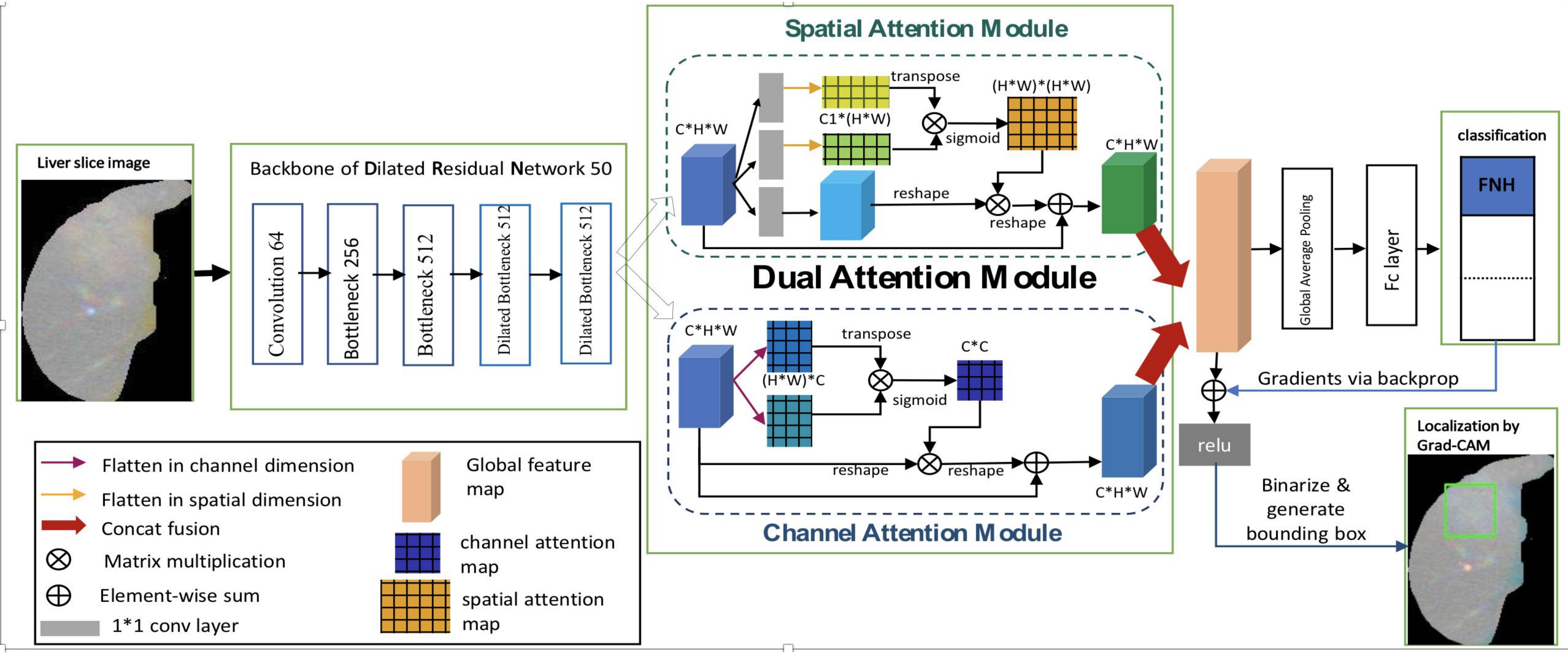

Methodology

Backbone Network

- Dilated Residual Network (DRN) (Yu et al. 2017)

DRN is chosen as the backbone classification network. Since the output of Group5 in DRN is <u>28*28</u>, which is much larger than that of original Resnet.

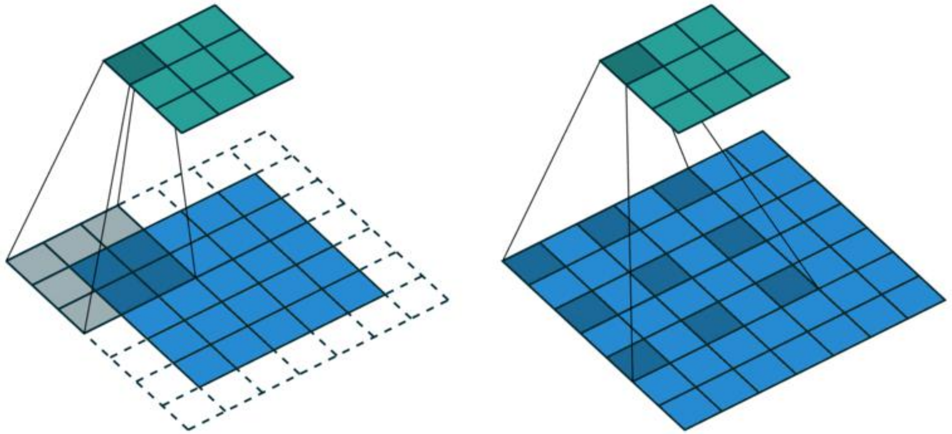

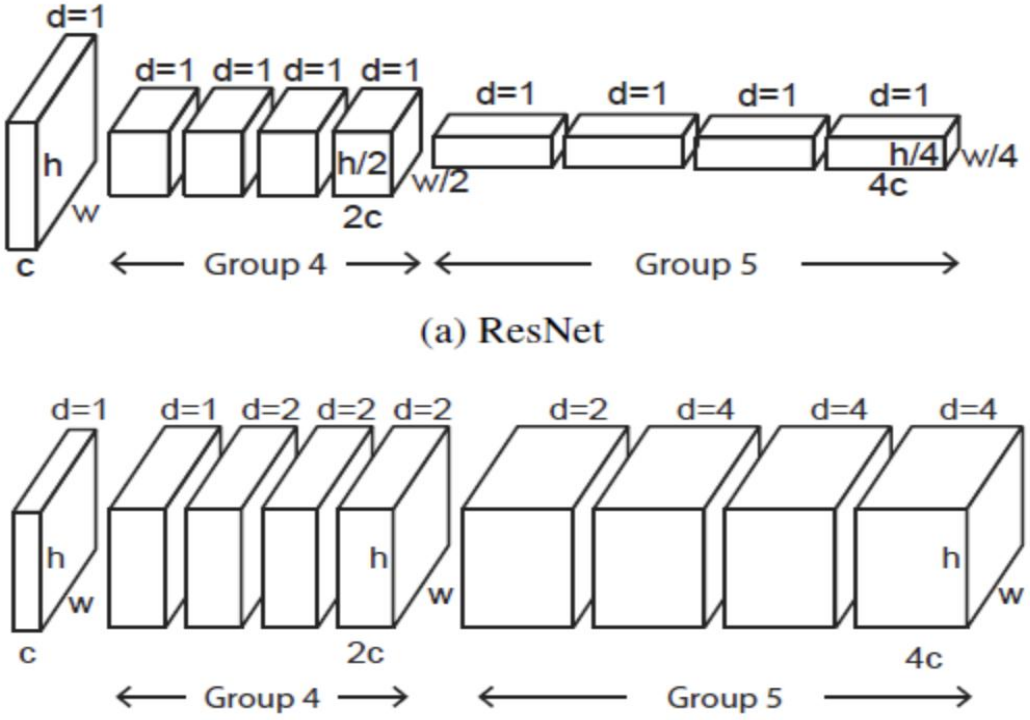

(a) ResNet

(b) DRN

Methodology

Visualization of Attention Maps

➢ Gradient-weighted Class Activation Maps (Grad-CAM) (Selvaraju et al. 2017)

$$L^{s}_{GradCAM} = ReLU\left(\sum_t \overbrace{\frac{1}{z}\sum_i\sum_j \frac{\partial y^s}{\partial A^k_{ij}}}^{GlobalAveragePooling} A^t\right)$$

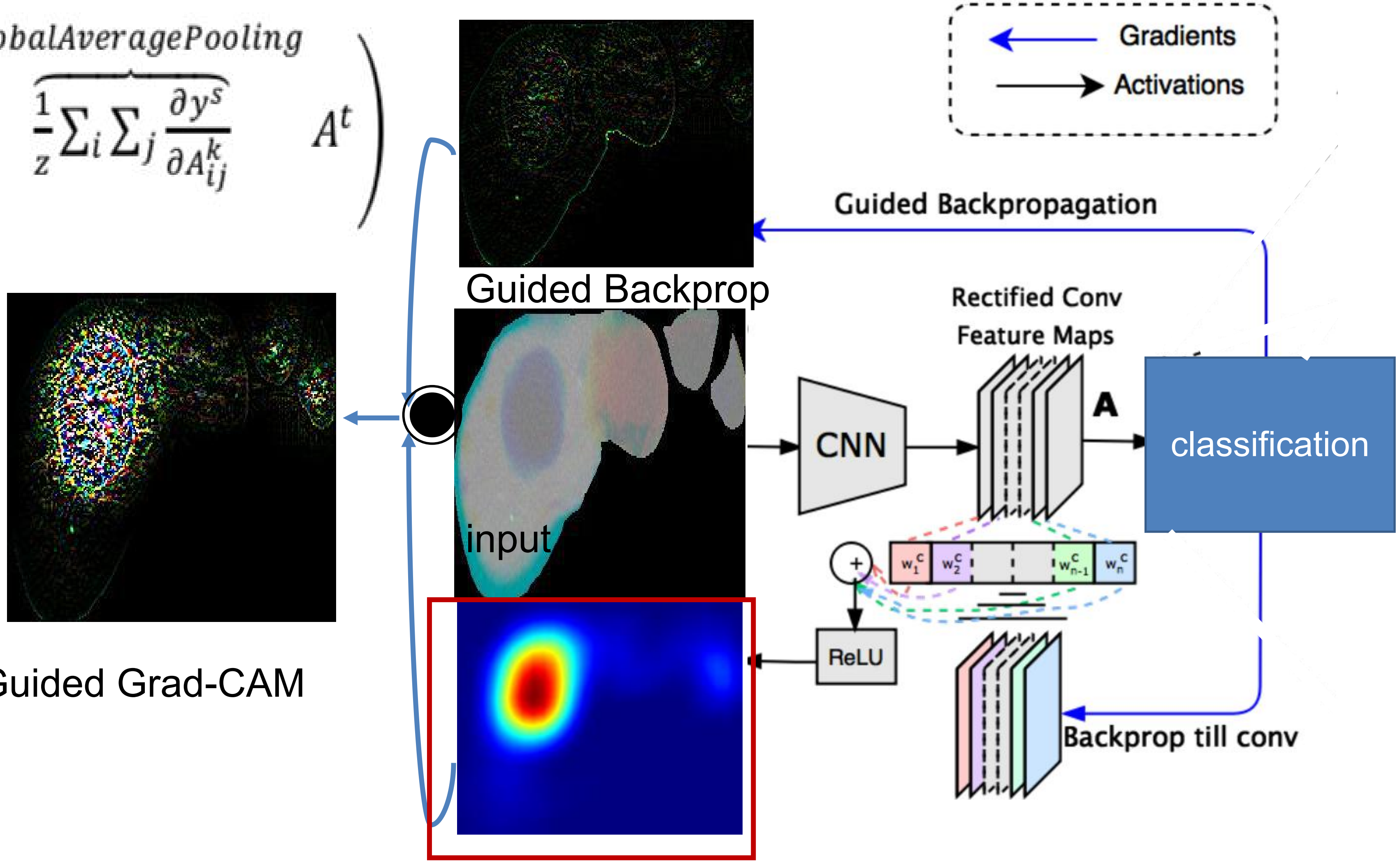

Content

Experiments

Dataset

A total of 1091 CT liver slice images in the arterial phase were included in our dataset, containing five types: normal, CYST, FNH, HCC and HEM. The data distribution is listed in **the following table**. To leverage 3D context information, each liver slice image contains two pieces of neighboring slice information on the z-axis. The input images were all resized to 224×224×3. To eliminate the effect of randomness, we split our dataset twice and the patient case did not overlap among the train set, validation set and test set.

Type	Train		Validation		Test		Total
	Set1	Set2	Set1	Set2	Set1	Set2	
Normal	135	126	41	57	51	44	227
CYST	168	166	56	59	69	68	293
FNH	75	75	29	27	26	28	130
HCC	149	143	52	57	50	51	251
HEM	112	114	38	37	40	39	190

Experiments

Comparison to other methods

Classification performance comparison with other attention-based CNN, baseline DRN, state-of-the-art ROI-level lesion classification method (ResGLNet).

1. Comparison of class-wise classification accuracy

Method	Normal	CYST	FNH	HCC	HEM
DRN50 [18]	0.9788	0.9327	0.7596	0.8427	0.5278
SEResnet50[14]	0.9334	0.9327	0.7788	0.9116	0.5917
RAResnet50[13]	0.9675	0.9182	0.7596	0.8227	0.5556
1 **SADRN50-A**	0.9577	0.9096	0.8132	0.8816	0.6625
SADRN50-B	0.9334	0.8761	0.7775	0.8220	0.5458
1 **CADRN50-A**	0.9675	0.9551	**0.8530**	0.9016	0.6181
CADRN50-B	0.9588	0.9413	0.8324	0.8322	0.5847
2 **DADRN50-A**	0.9690	0.9451	0.7802	0.8024	0.7069
DADRN50-B	**0.9804**	0.9551	0.8159	**0.9116**	0.6819
ResGLNet [21]	-	**0.9615**	0.8405	0.8846	**0.8462**

① Different normalization strategy in dual attention block: sigmoid(A) softmax(B)

② Different fusion strategy of spatial and channel attention: sum fusion(A) concatenate fusion(B)

Experiments

Comparison to other methods

Comparison of 5-class overall classification performance

Method	Accuracy	F1	Precision	Recall
DRN50 [18]	0.8083	0.8197	0.8294	0.8207
SEResnet50 [14]	0.8296	0.8265	0.8552	0.8149
RAResnet50 [13]	0.8047	0.8041	0.8304	0.7905
SADRN50-A	0.8449	0.8372	0.8463	0.8346
CADRN50-A	0.8591	0.8263	0.8506	0.8149
DADRN50-A	0.8407	0.8213	0.8446	0.8111
DADRN50-B	**0.8690**	**0.8412**	**0.8528**	**0.8386**

Experiments

Comparison to other methods

Weakly-supervised localization performance comparison with the state-of-the-art attention-based CNN and baseline DRN.

$$Localization\ Acc_c = \frac{total\ num\ of\ correct\ localized\ slices\ for\ class\ c}{total\ num\ of\ slices\ for\ class\ c}$$

Method	CYST	FNH	HCC	HEM
DRN50 [18]	0.5110	0.6676	0.5941	0.3798
SEResnet50 [14]	0.1898	0.0742	0.7327	0.2532
RAResnet50 [13]	0.2628	0.0742	0.6931	0.3292
DADRN50-B	**0.5986**	**0.6676**	**0.7327**	**0.5064**

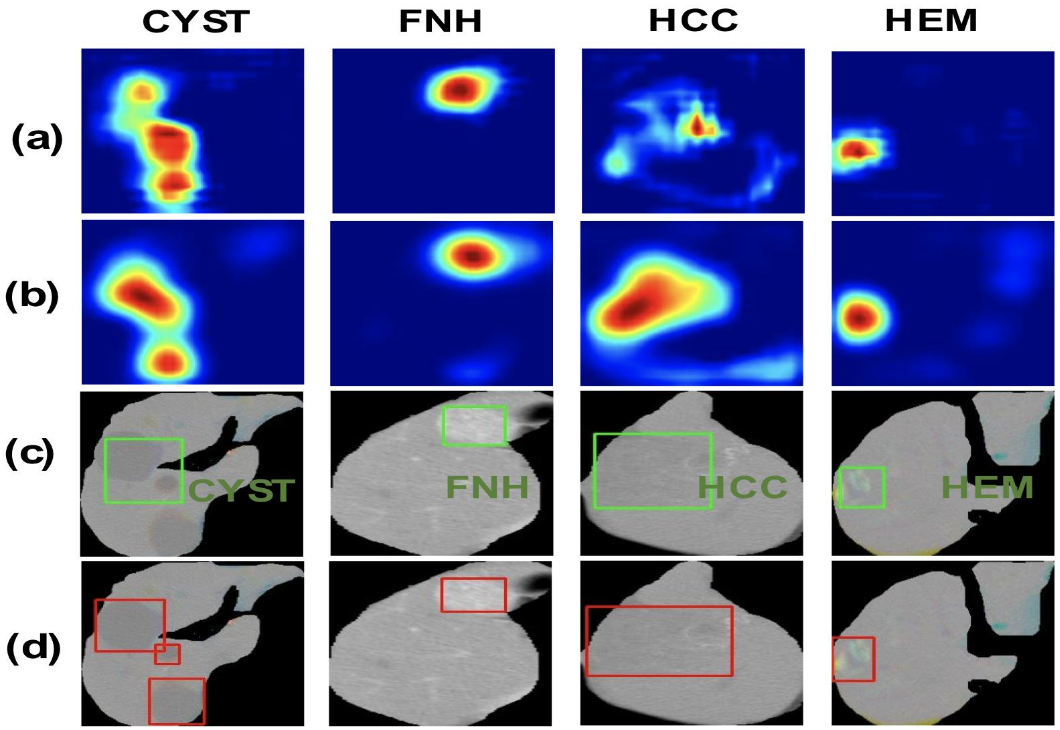

(a) Grad-CAM map of DRN; (b) Grad-CAM map of DADRN; (c) weakly-supervised localization result generated by (b); (d) ground truth of each slice image.

Content

Conclusion

- Dual attention module improve DRN’s lesion recognition ability
- DADRN is comparable to state-of-the-art ROI-level classification method and is superior to most state-of-the-art attention-based methods in lesion classification task and weakly-supervised lesion localization task.
- In future, we are going to develop a 3D attention-based network for 3D CT volumes to improve the classification accuracy. In addition, building a large scale liver lesions dataset remains a challenging task.

Thank you

RITSUMEIKAN